ACS chemical biology

Articles

pubs.acs.org/acschemicalbiology

A Blue-Absorbing Photolabile Protecting Group for *in Vivo* Chromatically Orthogonal Photoactivation

Ludovic Fournier,[†] Carole Gauron,[‡] Lijun Xu,[⊥] Isabelle Aujard,[†] Thomas Le Saux,[†,§] Nathalie Gagey-Eilstein,[†] Sylvie Maurin,[†] Sylvie Dubruille,[∥] Jean-Bernard Baudin,[†] David Bensimon,[⊥,¶] Michel Volovitch,[‡] Sophie Vriz,[‡] and Ludovic Jullien*[,†,§]

[†]Ecole Normale Supérieure, Département de Chimie, UMR CNRS-ENS-UPMC 8640 PASTEUR, 24, rue Lhomond, 75231 Paris Cedex 05, France

[‡]Collège de France, Center for Interdisciplinary Research in Biology (CIRB), CNRS, UMR 7241, INSERM, U1050, 11, Place Marcelin Berthelot, 75231 Paris Cedex 05, France

[⊥]Ecole Normale Supérieure, Département de Physique and Département de Biologie, Laboratoire de Physique Statistique, UMR CNRS-ENS 8550, 24 rue Lhomond, F-75231 Paris, France

[§]UPMC, 4, Place Jussieu, 75232 Paris Cedex 05, France,

[∥]Institut Curie, Centre de Recherche, CNRS, UMR 176, 26, rue d'Ulm, Paris F-75248, France

[¶]Department of Chemistry and Biochemistry, University of California, Los Angeles, Los Angeles, California, United States

Supporting Information

ABSTRACT: The small and synthetically easily accessible 7-diethylamino-4-thiocoumarinylmethyl photolabile protecting group has been validated for uncaging with blue light. It exhibits a significant action cross-section for uncaging in the 470−500 nm wavelength range and a low light absorption between 350 and 400 nm. These attractive features have been implemented in living zebrafish embryos to perform chromatic orthogonal photoactivation of two biologically active species controlling biological development with UV and blue-cyan light sources, respectively.

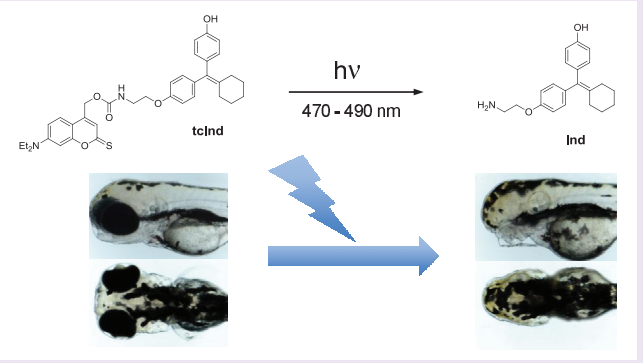

Photoactivation methods have recently proved attractive in various fields of chemistry and biology.[1−10] Among multiple photoactivation strategies, caged molecules have especially found a widespread use. These molecules rely on photolabile protecting groups that can be cleaved after light absorption by the photoactive moiety. In particular, they have been used to study the dynamics of several biological processes with high spatiotemporal resolution.[1−10] In such a context, one important constraint is to ensure that the illumination does not affect the biological system. This is particularly significant to discriminate the impact of the photoreleased substrate from the one of illumination (for instance during embryonic development[11,12]). This concern can be hardly fulfilled for living beings making extensive use of light to control their biological functions (photosynthetic procaryotes and plants for instance). However, it may be also relevant in a broader context since many endogenous biologically active molecules significantly absorb light even in the ultraviolet A range (UV A; 320−400 nm). Hence illumination of riboflavin or flavin mononucleotide (FMN) can photosensitize triplet dioxygen,[13] and the resulting singlet state $^1O_2$ can subsequently induce mitogen-activated protein kinases (MAPK) such as p38 and c-Jun-N-terminal kinase (JNK).[14,15] Carotenoids have been also incriminated since they are prone to UV A-induced photodegradation and are involved in the control of gene expression, either directly or via their $^1O_2$ quenching action.[16]

Most presently reported caging groups exhibit a maximum of wavelength absorption lying below the 450 nm range where riboflavin, FMN, and carotenoids absorb light.[1−10,17] To overcome this limit, a first strategy is to retain the established photochemistries with extension of the conjugation of the absorbing moiety. Depending on the series, this approach has met success[18,19] but has also exhibited limitations[20,21] when absorption red-shift was associated to a drop of the quantum yield for uncaging. The alternative strategy is to tailor caging groups based on chromophores absorbing in the visible range. This approach has been implemented by adapting the rearrangement of an amino-substituted 1,4-benzoquinone to

Received: March 13, 2013
Accepted: April 24, 2013
Published: May 7, 2013

Scheme 1. Syntheses of Caging Alcohol tcOH and Caged Inducer tcInd[a]

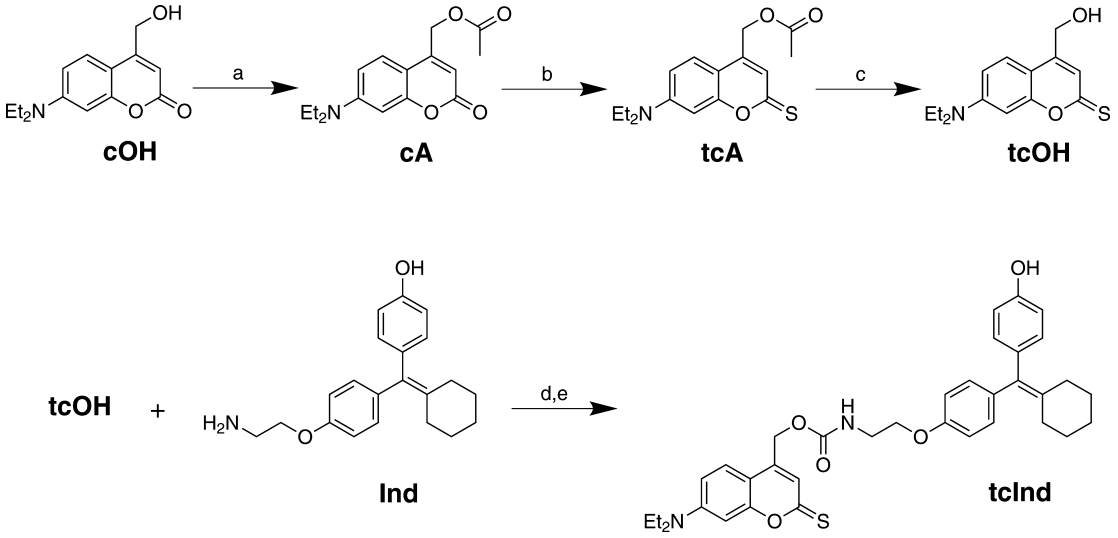

[a]Reagents and conditions: (a) acetic acid, DCC, DMAP, CH_2Cl_2, room temperature, 12 h; (b) Lawesson's reagent, toluene, reflux, 24 h; (c) 1.25 M HCl in ethanol, reflux, 15 h; (d) CDI, CH_2Cl_2, reflux, 4 h; (e) DMAP, CH_2Cl_2, reflux, 4 h.

photorelease carboxylic acids and phenols using visible light.[22,23] The xanthene chromophore has been used to photorelease carboxylates and phosphates upon illumination at 520 nm.[24] Ruthenium complexes have also been used to photorelease complexed amines.[25,26] We have chosen here to investigate the opportunities provided by the small and synthetically easily accessible thiocoumarin backbone.

Coumarins have led to the development of a successful series of synthetically easily accessible caging groups.[27−29] Considering that the light absorption of the thiocarbonyl group is significantly red-shifted with respect to the carbonyl analogue,[30,31] we have been interested in examining whether thiocoumarin analogues would exhibit a similar generic photochemical behavior[32−35] as suggested by the recent introduction of photocleavable protecting groups for carboxylic acids absorbing slightly below 400 nm.[36] In this work, we targeted the 7-diethylamino-4-methanol-thiocoumarin putative caging group, to benefit from its strongly donating substituent conjugated to the thiocarbonyl group to shift the wavelength of maximal absorption.

In this paper, we demonstrate that the 7-diethylamino-4-methanol-thiocoumarin moiety is a relevant blue-absorbing caging group, which can be used in living zebrafish embryos in the context of developmental biology. Relying on a caged cyclofen-OH[37,38] analogue, we were able to photocontrol with blue light the activity of a transcription factor (En2) fused to the modified estrogen receptor ligand-binding domain ER^{T2}.[39,40] Moreover, taking advantage of the low absorption of 7-diethylamino-4-methanol-thiocoumarin in the 350−400 nm wavelength range, we used two different wavelengths (365 and 488 nm) to orthogonally photoinduce[41−47] two distinct phenotypes upon independently photogenerating two biologically active substrates: an analogue of the previously investigated cyclofen-OH[37,38] and 13-*cis*-retinoic acid (13-*cis*-RA).

RESULTS AND DISCUSSION

Thiocoumarins can be obtained in good yields in one step from the corresponding coumarins using the Lawesson's reagent.[48−51] Our syntheses are shown in Scheme 1. Starting from the commercially available 7-diethylamino-4-methylcoumarin, we first prepared the 7-diethylamino-4-hydroxymethylcoumarin **cOH** in a one-pot process in 42% yield, upon adapting reported two-step procedures (SeO_2, dioxane/water, reflux, 14 days; $NaBH_4$, ethanol, RT, 12 h).[52,53] The alcohol **cOH** was then esterified with acetic acid using the *N*,*N*′-dicyclohexylcarbodiimide (DCC) coupling reagent to yield the ester **cA** with 85% yield. This ester was subsequently converted into the corresponding thiocoumarin **tcA** (Lawesson's reagent, toluene, reflux, 24 h) in 92% yield. The thiocoumarin **tcA** was eventually hydrolyzed (1.25 M HCl in ethanol, reflux, 15 h) to provide the putative caging alcohol **tcOH** with 75% chemical yield (see Supporting Information).

To evaluate the relevance of the present caging group, we adopted a substrate acting as an inducer for controlling the activity of target proteins fused to the extensively used modified estrogen receptor ligand-binding domain (ER^{T2}) specific for the non-endogenous 4-hydroxy-tamoxifen inducer.[39,40] Relying on an extensive study of the relationship between inducer structure and function,[54] we targeted an analogue of the previously investigated cyclofen-OH,[37,38] which is denoted **Ind** in the following (Scheme 1). **Ind** contains a terminal primary amino moiety,[55] to be engaged in the carbamate group, which has been widely used for caging in the coumarin series for biological purposes.[27] **Ind** was easily synthesized in three steps from 4-[cyclohexylidene(4-hydroxyphenyl)methyl]-phenol (see Supporting Information).[37,38] The caged inducer **tcInd** was eventually obtained in 30% yield by condensing **Ind** on the carbamate intermediate resulting from reaction between *N*,*N*′-carbonyldiimidazole and **tcOH**.

tcInd is thermally stable at the day time scale in 20 mM pH 7.5 Tris buffer/acetonitrile 1/1 (v/v) at RT. Its solution strongly absorbs light in the visible range: A maximum of absorption originating from the thiocoumarin chromophore is observed at λ_{max}(**tcInd**) = 469 nm (ε_{tcInd}(469 nm) = 2.7×10^4 M^{-1} cm^{-1}), and its molar absorption coefficient remains larger than 1.0×10^4 M^{-1} cm^{-1} beyond 500 nm (Figure 1a). Its molar absorption is also interestingly 10 times lower (~3×10^3 M^{-1} cm^{-1}) in the 350−400 nm range than at its maximal absorption. In addition, **tcInd** is only weakly fluorescent upon excitation at

dx.doi.org/10.1021/cb400178m | ACS Chem. Biol. 2013, 8, 1528−1536

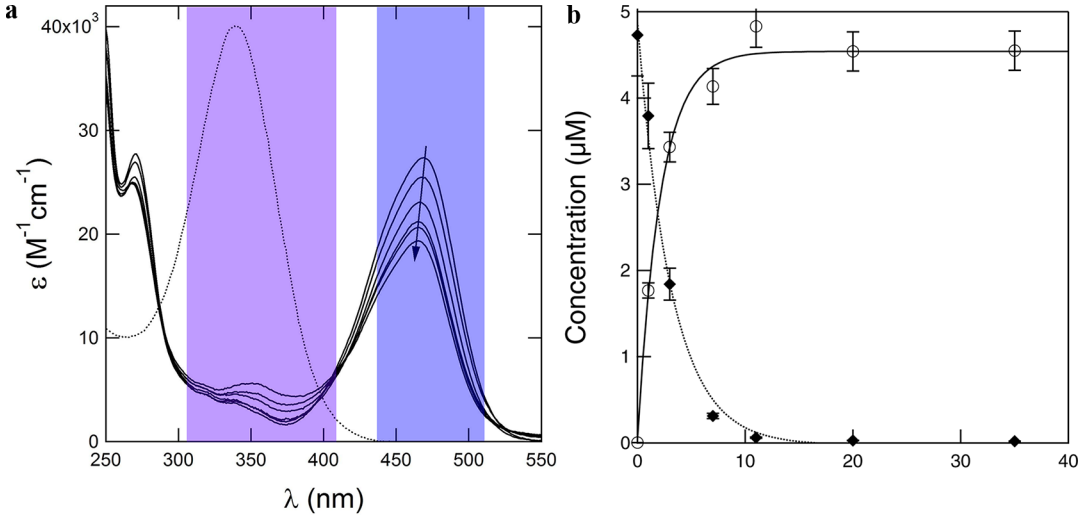

Figure 1. Evolution of the composition of a 5 μM **tcInd** solution in 20 mM pH 7.5 Tris buffer/acetonitrile (v/v) upon illumination at 470 nm for various durations t ($\mathcal{I}_0(470) = 2.2 \times 10^{-8}$ einstein s^{-1} cm^{-2}). (a) Temporal evolution of the solution absorbance normalized to its concentration to afford its molar absorption coefficient $\varepsilon(\lambda)$ (t = 0, 1, 3, 7, 11, 20 min; solid line). The absorption spectrum of 13-*cis*-RA (to be used below as a photoactive precursor) is shown as a dotted line, and the wavelength ranges of the UV and blue light sources used for embryo illumination as violet and blue zones, respectively. (b) Temporal evolution of the concentrations in **tcInd** (diamonds) and **Ind** (circles) extracted from the peak areas in the HPLC chromatogram. Markers: experimental data. Lines: exponential fits $[\mathbf{tcInd}]_t = [\mathbf{tcInd}]_0\ e^{-k_u t}$ (dotted) and $[\mathbf{Ind}]_t = [\mathbf{Ind}]_\infty(1 - e^{-k_u t})$ (solid). The fits provide $[\mathbf{tcInd}]_0 = 4.9 \pm 0.1$ μM and $[\mathbf{Ind}]_\infty = 4.5 \pm 0.2$ μM, and 0.5 ± 0.1 and 0.3 ± 0.1 for k_u expressed in min^{-1}. T = 293 K.

λ_{exc} = 470 nm. We estimated its quantum yield of light emission to be Φ_{em}(**tcInd**) = 1% with a maximum at λ_{em}(**tcInd**) = 550 nm. Since the **tcOH** alcohol resulted from **tcInd** uncaging (*vide infra*), we also examined the **tcOH** photophysical features. As anticipated from the similarity of the chromophores in both compounds, the alcohol **tcOH** exhibits a similar photophysical behavior. In the same solvent, we observed λ_{max}(**tcOH**) = 467 nm (ε_{tcOH}(467 nm) = 2.4×10^4 M^{-1} cm^{-1}), λ_{em}(**tcOH**) = 551 nm (Φ_{em}(**tcOH**) = 1%).

We illuminated a 5.0 ± 0.2 μM **tcInd** solution in 20 mM pH 7.5 Tris buffer/acetonitrile (v/v) with blue light in order to evidence any photorelease of the inducer. Aliquots of the **tcInd** solution illuminated at 470 nm for increasing durations were analyzed both by HPLC–mass spectrometry and UV–vis absorption. Analyses of HPLC retention times and of mass spectra with original samples first demonstrated that illumination converted **tcInd** into **Ind** and the alcohol **tcOH**. We analyzed the evolutions of the concentrations of **tcInd** and **Ind** as a function of the illumination duration (Figure 1b). As expected, the concentration of the photoproduct increased with time and converged toward the concentration range of the initial **tcInd** solution (5 μM); we estimated the final concentration in photoreleased inducer **Ind** to be 4.5 ± 0.2 μM. Meanwhile **tcInd** concentration exponentially decayed toward zero. These observations suggest that uncaging was essentially quantitative. Moreover the exponential decays allowed us to extract two independent estimates of the rate constant k_u associated to **tcInd** photoactivation after one-photon excitation (see Methods). From the data associated with **tcInd** and **Ind**, we derived, respectively, 0.5 ± 0.1 and 0.3 ± 0.1 min^{-1}. These results were further confirmed by analyzing the temporal evolution of the absorption spectrum of the **tcInd** solution. Figure 1a shows that the absorbance in the visible range blue-shifted from 469 to 465 nm upon increasing the illumination duration. Since the photoreleased inducer did not contribute to the absorbance in the corresponding wavelength range, it was noticeable that the maximal absorption of the illuminated **tcInd** solution asymptotically shifted toward the maximal absorption of the reference alcohol **tcOH**. However, we also noticed that the molar absorption dropped below that expected for **tcOH**. Indeed HPLC evidenced that **tcOH** photodegraded at the longest times (see Supplementary Figure 1S). From the exponential decay of the normalized absorbance at the shortest times, we derived another independent estimate of k_u = 0.3 ± 0.1 min^{-1}, in reasonable agreement with the previous values. After calibration of the photon flux at the sample, we extracted the quantum yield and the action cross-section with one-photon excitation associated to **tcInd** photoconsumption leading to **Ind** liberation. We found $\Phi_{tcInd}(470) = 5 \pm 1 \times 10^{-3}$ and $\varepsilon_{tcInd}(470)\Phi_{tcInd}(470) = 120 \pm 25$ M^{-1} cm^{-1} at λ_{max} = 470 nm respectively. Such values were in the range typically observed for the widely used 4,5-dimethoxy-2-nitrobenzyl caging group (respectively, 6×10^{-3} and 48 M^{-1} cm^{-1} at 350 nm in ref 20), but with an absorption range significantly red-shifted by 120 nm. They also notably exceeded by more than 1 order of magnitude the uncaging efficiency at 470 nm of the popular diethylaminocoumarin photolabile moiety.[47]

After evidencing **tcInd** uncaging *in vitro*, we evaluated the relevance of this system *in vivo*. We chose to photocontrol in developing zebrafish embryos the function of En2, a well-established cell-autonomous transcription factor,[56] which is a key element in the formation of the diencephalic-mesencephalic boundary (DMB) in zebrafish. En2 overexpression moves the DMB rostrally, whereas En2 knockdown moves the DMB caudally.[57] For example, En2 overexpression induces a reduction of the size of the diencephalon, which results in a reduction of the size or a total absence of eyes (Figure 2a).[58] We injected the mRNA coding for the En2-ER^{T2} fusion protein at the one-cell stage in zebrafish embryos. We then attempted to induce overexpression of En2 activity at 70% epiboly (epiboly is a cell movement occurring in the early embryo) by adding **Ind** or by photoactivating its caged precursor **tcInd** with blue light. With respect to control embryos developing in the

dx.doi.org/10.1021/cb400178m | *ACS Chem. Biol.* 2013, 8, 1528–1536

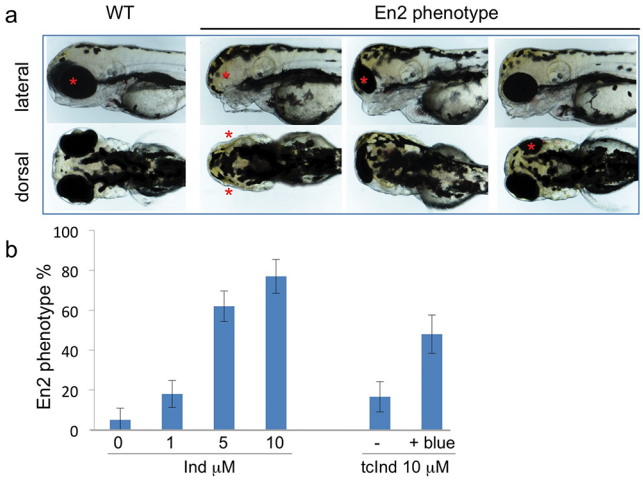

Figure 2. Photoactivation of **tcInd** by blue illumination in En2-ER^{T2} mRNA-injected embryos ($\mathcal{I}_0(470) = 3.2 \times 10^{-8}$ einstein s^{-1} cm^{-2}). (a) En2 positive phenotype (absent or reduced eye; red stars were introduced to identify important structures) observed in lateral and dorsal views of three embryos at 72 hpf after uncaging of **tcInd** (10 μM) in the presence of (2-hydroxypropyl)-β-cyclodextrin (10 μM). Untreated wild type embryos are displayed on the left as controls. The corresponding wild type phenotype was similarly observed at 83% for non-illuminated En2-ER^{T2} mRNA-injected embryos. (b) Percentage of positive En2 phenotype observed in incubating solutions containing various **Ind** concentrations (left) or 10 μM **tcInd** photoactivated with blue light for 10 min in the presence of 10 μM (2-hydroxypropyl)-β-cyclodextrin (right).

absence of inducer, we first checked that zebrafish embryos did not exhibit any significant abnormal development when incubated in various **Ind** concentrations (up to 10 μM). We then examined En2-ERT2-injected zebrafish embryos. In the absence of inducer, the embryos displayed a normal phenotype at 72 h post fertilization (hpf): no difference could be observed between non-injected embryos and embryos injected with En2-ER^{T2} mRNA (Figure 2a). In contrast, upon incubation in a medium containing the inducer, the percentage of embryos with eye defect (heterogeneous phenotype from complete absence of eye to reduction of eye size) increased, reaching 50% at an inducer concentration $Ind_{1/2} = 3 \pm 1$ μM (Figure 2a and Supplementary Table 1S). Equipped with this information, we exposed En2-ER^{T2}-injected zebrafish embryos to a 10 μM **tcInd** solution in the presence of 10 μM (2-hydroxypropyl)-β-cyclodextrin added to achieve embryo perfusion with the caged inducer (see Supporting Information).[59] In the absence of blue illumination, we observed a three times higher incidence of En2 phenotype than in the control without caged inducer (Figure 2b), which probably originated from some partial thermally driven **tcInd** hydrolysis after 3 days of incubation. However, such a leakage was not detrimental to considerably increase the incidence of En2 phenotype, when **tcInd** was illuminated by blue light for a duration similar to its uncaging time (Figure 2b). More precisely, the embryos displayed the characteristic positive phenotype they showed in the presence of similar concentrations of the free inducer upon taking into account that half of the photoreleased **Ind** molecules remained trapped within (2-hydroxypropyl)-β-cyclodextrin after uncaging so as to reduce the concentration in free inducer for embryo perfusion (see Supporting Information).

After validation of **tcInd** photoactivation by blue light *in vivo*, we have been interested in exploiting the major red shift of the thiocoumarin chromophore to orthogonally photogenerate two biologically active substrates with two different wavelengths.[41−47] Besides **tcInd** photoactivation by blue light, we chose to photoactivate 13-*cis*-retinoic acid (13-*cis*-RA) by UV (365 nm) light, a wavelength range that is extensively used for uncaging in a biological context. Indeed we recently showed that 13-*cis*-RA illumination close to its absorption maximum (see Figure 1a) caused its photoisomerization into all-*trans*-retinoic acid (all-*trans*-RA),[12] leading to rescue of hindbrain formation in embryos whose all-*trans* RA synthetic pathway had been impaired by adding diethylaminobenzaldehyde (DEAB) as an inhibitor (see Supplementary Figure 2S).[60] More specifically, rescue was evidenced upon photoactivating 13-*cis*-RA at 90% epiboly in a transgenic line, which expressed green fluorescent protein (GFP) both in the third (r3) and in the fifth (r5) rhombomeres. Using the ratio of total fluorescence from r5 with respect to r3, we showed that r5 development was restored only after UV illumination.

In a first step, we evaluated *in vitro* whether we could observe preferential photoactivation of **tcInd** (respectively, 13-*cis*-RA) upon illuminating at 488 (respectively, 365) nm. Hence we submitted separate 10 μM solutions of **tcInd** and 13-*cis*-RA in 20 mM pH 7.5 Tris buffer/acetonitrile 1/1 (v/v) either to 5 min of 488 nm or/and 1 min of 365 nm illumination at RT. The resulting concentrations in photoreleased inducer **Ind** and all-*trans*-RA are displayed in Figure 3a and Supplementary Table 5S. Five minutes of 488 nm illumination liberated 6.5 μM **Ind** without simultaneously generating any significant amount of all-*trans*-RA. On the other hand, 1 min of 365 nm illumination yielded about 3 μM all-*trans*-RA, which amounted to 30% yield, in quantitative agreement with our previous 25−30% results.[12,60] At the same time we observed the formation of 0.75 μM **Ind**, which allowed us to extract the quantum yield of **tcInd** photoconsumption at 365 nm, $\Phi_{\mathbf{tcInd}}(365) = 6 \times 10^{-3}$, in close agreement with the value upon illuminating at 470 nm. In fact, the observed orthogonal photogeneration of both biologically active substrates with 365 and 488 nm wavelengths was in quantitative agreement with the calculated ratio of the photoactivation cross-sections of **tcInd** and 13-*cis*-RA at 488 and 365 nm. Indeed, retaining $\Phi_{\mathbf{tcInd}} = 5 \times 10^{-3}$ and $\Phi_{13cisRA} = 1.5 \times 10^{-2}$ (ref 61) for the quantum yields of photoactivation of **tcInd** and 13-*cis*-RA at 488 and 365 nm, respectively, we derived from absorption spectra $[\varepsilon_{\mathbf{tcInd}}(488)\Phi_{\mathbf{tcInd}}]/[\varepsilon_{13cisRA}(488)\Phi_{13cisRA}] > 100$ and $[\varepsilon_{13cisRA}(365)\Phi_{13cisRA}]/[\varepsilon_{\mathbf{tcInd}}(365)\Phi_{\mathbf{tcInd}}] \simeq 50$.

After the latter *in vitro* validation, we incubated transgenic embryos injected with the mRNA of En2-ER^{T2} in a medium containing 10 μM DEAB, 10 μM **tcInd**, and 5 nM 13-*cis*-RA (see Supporting Information). We subsequently submitted these embryos either to 5 min of 488 nm[62] or/and 1 min of 365 nm illumination (see Figure 1a). The results are displayed in Figure 3b−f and Supplementary Table 6S. In the absence of any illumination, we essentially observed neither size reduction or loss of eye (positive En2 phenotype) nor r5 rescue (positive all-*trans*-RA phenotype) (Figure 3b). In contrast, when the embryos were illuminated by blue light, we observed the characteristic **tcInd** photoinduced positive phenotype without interference with the 13-*cis*-RA one (Figure 3c); more precisely, we observed the En2 phenotype level in the range expected upon photoreleasing 6.5 μM **Ind**, yielding 3.5 μM free inducer available for its biological activity upon using 1.2×10^5 for **Ind** association constant to the cyclodextrin (see Supporting Information). Conversely, when the embryos were illuminated

dx.doi.org/10.1021/cb400178m | ACS Chem. Biol. 2013, 8, 1528−1536

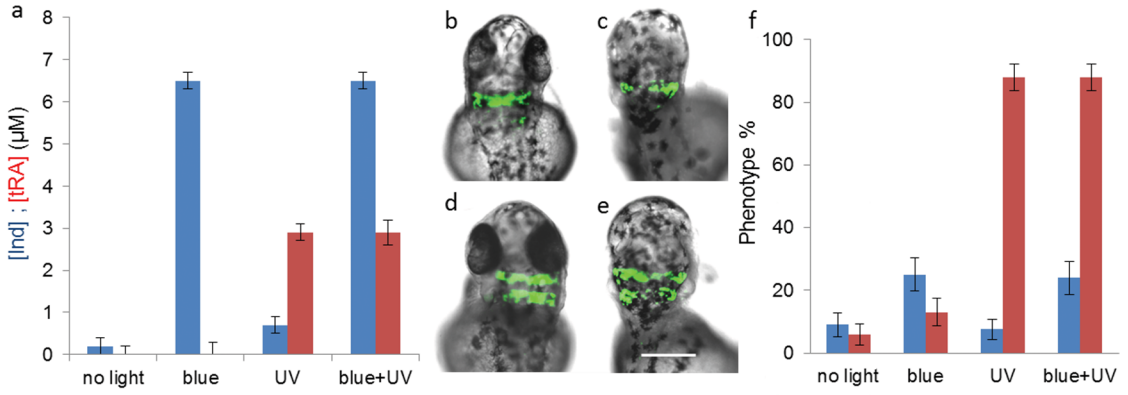

Figure 3. (a) Concentrations in photoreleased inducer **Ind** and all-*trans*-RA after either 5 min blue (488 nm) or/and 1 min UV (365 nm) illumination of separate 10 μM solutions of **tcInd** and 13-*cis*-RA in 20 mM pH 7.5 Tris buffer/acetonitrile 1/1 (v/v) at RT. Red bar: all-*trans*-RA. Blue bar: **Ind**. (b−e) En2- and all-*trans*-RA-induced phenotypes in En2-ER^{T2} mRNA-injected mp311+/+GFP embryos conditioned with **tcInd** (10 μM) and 13-*cis*-RA (5 nM) in a medium containing 10 μM DEAB subsequently submitted to 488 nm (c), 365 nm (d), and 365 and 488 nm illumination (e) ($\mathcal{I}_0(488) = 8.6 \times 10^{-8}$ einstein s^{-1} cm^{-2}) and $\mathcal{I}_0(365) = 3.0 \times 10^{-8}$ einstein s^{-1} cm^{-2}). A non-illuminated embryo at 48 hpf is displayed in panel b. One observes the following: in panel b, the eyes (no En2 overexpression) and no r5 (no all-*trans*-RA); in panel c, no eyes (blue light photogenerated En2 overexpression) and no r5 (no all-*trans*-RA); in panel d, the eyes (no En2 overexpression) and r5 (UV light photogenerated all-*trans*-RA); in panel e, no eyes (blue light photogenerated En2 overexpression) and r5 (UV light photogenerated all-*trans*-RA). Scale bar = 500 μm. (f) Percentages of positive phenotypes resulting from photoactivation of **tcInd** and 13-*cis*-RA by 488 and 365 nm illuminations in En2-ER^{T2} mRNA-injected mp311+/+GFP zebrafish embryos in a medium containing 10 μM DEAB. Blue bar: positive En2 phenotype. Red bar: positive all-*trans*-RA phenotype.

by UV light, they exhibited the 13-*cis*-RA photoinduced positive phenotype without any interference with the **tcInd** one (Figure 3d); more precisely, the phenotype levels were in line with the photogeneration of 30% of all-*trans*-RA from 5 nM 13-*cis*-RA (1.5 nM generates 90% of positive phenotype; see ref 60) and 0.75 μM **Ind** (e.g., 0.35 μM uncomplexed **Ind**) from 10 μM **tcInd**. The achievement of the orthogonally chromatic photoactivation was further emphasized by analyzing the phenotype observed upon applying both blue and UV illuminations (Figure 3e), which distinctly evidenced positive phenotypes induced by photogeneration of **Ind** and all-*trans*-RA.

Concluding Remarks. The 7-diethylamino-4-thiocoumarinylmethyl moiety exhibits attractive features as a caging group. It is synthetically easily accessible, exhibits a significant action cross-section for uncaging in the blue wavelength range ($\varepsilon_{\mathbf{tcInd}}(470)\Phi_{\mathbf{tcInd}}(470) = 120 \pm 25$ M^{-1} cm^{-1}), and has been validated in a biological context. Moreover its low action cross-section for uncaging in the 350−400 nm wavelength range ($\varepsilon_{\mathbf{tcInd}}(365)\Phi_{\mathbf{tcInd}}(365) = 12 \pm 2$ M^{-1} cm^{-1}) makes it attractive to perform chromatic orthogonal uncaging in combination with many presently available UV-absorbing caging groups, which do not exhibit any significant absorption beyond 450 nm. Indeed such a value remains significantly lower than the action cross-section for uncaging of even modestly efficient UV-absorbing caging groups,[1−10] so as to avoid any major 7-diethylamino-4-thiocoumarinylmethyl photoactivation when UV illumination is applied. In particular, the 7-diethylamino-4-thiocoumarinylmethyl caging group could be used to orthogonally photorelease one or two biologically active species with a variable delay in different territories, thus opening a way to analyze self- and cross-feedbacks during embryo development, both in time and space.

METHODS

Syntheses. The experimental subsection reporting on the syntheses is in the Supporting Information.

Reagents and Solutions. Tris base (2-amino-2-(hydroxymethyl)-1,3-propanediol 99.8+% A.C.S. reagent) and acetonitrile (spectrophotometric grade) were from Sigma-Aldrich. All solutions were prepared using water purified through a Direct-Q 5 (Millipore, Billerica, MA). All *in vitro* experiments were performed at 293 K in a buffered solution obtained by mixing in equal volumes acetonitrile and a 20 mM Tris base aqueous solution acidified to 7.5 (measured with a pH meter PHM 210; Radiometer Analytical calibrated at pH = 4 and 7) with 1 M chlorhydric acid.

Photophysical Properties. The UV−vis absorption spectra were recorded at 293 K either on a Kontron Uvikon-940 having cell holders thermostatted with a circulating bath (Polystat 34-R2, Fisher Bioblock Scientific, Illkirch, France) or on a Agilent Cary 300 spectrophotometer equipped with 1 × 1 cm^2 Peltier cell holders. Molar absorption coefficients were extracted while checking the validity of the Beer−Lambert law.

Corrected emission spectra upon one-photon excitation were obtained from a Photon Technology International QuantaMaster spectrofluorimeter having a Peltier thermostatted cell holder (TLC50, Quantum Northwest, USA). Solutions for emission measurements were adjusted to concentrations such that the absorption maximum was around 0.15 at the excitation wavelength. The overall emission quantum yields after one-photon excitation Φ_{em} were calculated from the relation

$$\Phi_{em} = \Phi_{ref}\frac{1 - 10^{-A_{ref}(\lambda_{exc})}}{1 - 10^{-A(\lambda_{exc})}}\frac{D}{D_{ref}}\left(\frac{n}{n_{ref}}\right)^2 \quad (1)$$

where the subscript ref stands for standard samples. $A(\lambda_{exc})$ is the absorbance at the excitation wavelength, D is the integrated emission spectrum, and n is the refractive index for the solvent. The uncertainty in the experimental value of Φ_{em} was estimated to be ±10%. The standard fluorophore for the quantum yields measurements was Fluoresceine in sodium hydroxide 0.1 M with $\Phi_{ref} = 0.92$.[63]

The quartz cuvettes (Hellma) were 1 cm × 1 cm (3 mL samples). The temperature was directly measured in the cuvettes using a type K thermocouple connected to a ST-610B digital pyrometer (Stafford Instruments, Stafford, U.K).

HPLC Coupled to Mass Spectrometry. High pressure liquid chromatography was carried out with an Accela System liquid chromatograph (Thermo Finnigan, Les Ulis, France) equipped with a Hypersil Gold column (1.9 μm, 2.1 mm × 50 mm) connected to a

dx.doi.org/10.1021/cb400178m | ACS Chem. Biol. 2013, 8, 1528−1536

Thermo-Finnigan TSQ Quantum Discovery Max triple quadrupole mass spectrometer. Five microliters of illuminated sample solution was injected in the chromatographic column. The analytes eluted from the column with a mobile phase composed of two solvents A (water containing formic acid at 0.05% v/v) and B (acetonitrile). A gradient was used to optimize the separation of the analytes. Initially, the column was equilibrated at 0.20 mL min^{-1} with a mobile phase consisting of 90% A and 10% B. One minute after injection, the proportion of B was linearly increased to 80% within 4 min and remained at that proportion for an additional 2 min. After this step, composition of the mobile phase was set to initial conditions, and the column was equilibrated for 3 min prior to the next injection. Detection was performed by mass spectrometry. After separation, the analytes were introduced in the mass spectrometer through a heated electrospray ionization source (50 °C, 4000 V) operating in the positive mode. The temperature of the capillary transfer was set at 270 °C. Nitrogen was employed as nebulizing (35 psi) and auxiliary gas (30 arbitrary units). Argon was used as collision gas (1.0 mTorr in Q2). Peak areas were converted into concentrations after preliminary calibrations. Instrument control and data collection were handled by a computer equipped with Xcalibur software (version 2.0).

Irradiation Experiments. Two different protocols have been used to perform the irradiations.

In cuvettes. Illumination Experiments. The experiments devoted to the identification of the photoproducts and to the analysis of photoconsumption kinetics were performed at 5 μM concentration on 3 mL samples in 1 × 1 cm^2 quartz cuvettes under constant stirring. Excitation at 470 nm was performed with the 75 W xenon lamp of the spectrofluorometer. After each illumination delay, 200 μL were removed for subsequent analysis with HPLC/Mass spectrometry.

The 470 nm overall incident light intensity, $I_0(470)$, was calibrated using a procedure relying on analyzing the intensity I_{DCM} of fluorescence emission of a 4-dicyanomethylene-2-methyl-6-*p*-dimethylamino-styryl-4*H*-pyrane (DCM) solution in absolute ethanol upon exciting at two different wavelengths. The fluorescence emission $I_{DCM}(470)$ associated with $I_0(470)$ was first recorded upon exciting at 470 nm where DCM absorbs light with molar absorption coefficient $\varepsilon_{DCM}(470)$. Then the corresponding fluorescence emission $I_{DCM}(365)$ was recorded upon exciting at 365 nm with light intensity $I_0(365)$ (molar absorption coefficient $\varepsilon_{DCM}(365)$). $I_0(365)$ was subsequently extracted from determining the kinetics of photoconversion at 365 nm of the α-(4-dimethylaminophenyl)-*N*-phenylnitrone into 3-(4-dimethylaminophenyl)-2-phenyloxaziridine in absolute ethanol as described in reference 64. Eventually, the blue light intensity $I_0(470)$ was computed from $[\varepsilon_{DCM}(365)I_{DCM}(470)]/[\varepsilon_{DCM}(470)I_{DCM}(365)]$. The surfacic photon flux $\mathcal{I}_0(470)$ was then derived from dividing the 470 nm overall incident light intensity $I_0(470)$ by the cuvette surface (3 cm^2). During the present series of experiments, typical overall and surfacic photon fluxes at the sample were in the 10^{-7} einstein s^{-1} and 2 × 10^{-8} einstein s^{-1} cm^{-2} ranges, respectively.

Extraction of the Photochemical Parameters. Assuming that photoactivation is rate-limiting among the processes leading to SH liberation, we considered that the illuminated system was submitted to the reaction

$$\mathrm{SPG} \xrightarrow{h\nu} \mathrm{SH} + \mathrm{PG} \tag{2}$$

to derive the cross-section for **tcInd** photoconsumption after one-photon excitation. In eq 2, SPG, SH, and PG designate the caged species, the species that was initially caged, and the product from the protecting moiety after SH release. The reaction rate for the photoconsumption of the caged compound SPG is proportional to the intensity of the monochromatic excitation light absorbed by SPG at the excitation wavelength, $I_u(\lambda_{exc})$ and to the photoconsumption cross-section with one-photon excitation, ϕ_u:

$$-\frac{\mathrm{d}[\mathrm{SPG}]}{\mathrm{d}t} = \frac{I_u(\lambda_{exc})\phi_u}{V} \tag{3}$$

where V is the irradiated volume and $I_u(\lambda_{exc})$ is expressed in einstein per unit of time. Provided that the total absorbance at the excitation wavelength is much lower than 1, one obtains at first order[64]

$$[\mathrm{SPG}] = [\mathrm{SPG}]_0 \exp(-k_u t) \tag{4}$$

with

$$k_u = \frac{2.3\phi_u I_0(\lambda_{exc})\varepsilon_u(\lambda_{exc})l}{V} \tag{5}$$

where $[\mathrm{SPG}]_0$ is the initial concentration in caged species, and $\varepsilon_u(\lambda_{exc})$ and l are the effective molar absorption coefficient for photoconsumption of SPG at the excitation wavelength and the path length of the light beam, respectively. By assuming that the system initially contains only SPG, one then easily derives

$$\frac{A_{tot}(\lambda_{exc}, t)}{A_{tot}(\lambda_{exc}, 0)} = \frac{\varepsilon_{SH}(\lambda_{exc}) + \varepsilon_{PG}(\lambda_{exc})}{\varepsilon_{SPG}(\lambda_{exc})} + \left(1 - \frac{\varepsilon_{SH}(\lambda_{exc}) + \varepsilon_{PG}(\lambda_{exc})}{\varepsilon_{SPG}(\lambda_{exc})}\right)\exp(-k_u t) \tag{6}$$

where ε_{SH}, ε_{PG}, and ε_{SPG} designate the molar absorption coefficients of SH, PG, and SPG respectively.

Exponential fit of experimental data yielded k_u, from which we extracted the action cross-section with one-photon excitation associated with **tcInd** photoconsumption:

$$\varepsilon_u(\lambda_{exc})\phi_u(\lambda_{exc}) = \frac{k_u V}{2.3 l I_0} \tag{7}$$

The associated quantum yield $\phi_u(\lambda_{exc})$ was eventually obtained using the value of the molar absorption of the caged inducer from its absorption spectrum.

In Dishes Containing Zebrafish Embryos. One-photon illumination experiments were also performed at 20 °C. Three light sources have been used:

- a blue light source (470 nm LED, essentially a 40 nm wide, at half height, Gaussian distribution centered at 470 nm; LXML-PB01, Philips Lumileds, San Jose, CA) delivering typical 3 × 10^{-8} einstein s^{-1} cm^{-2} surfacic photon fluxes $\mathcal{I}_0$ at the illuminated sample. It was used for the blue illumination experiments involving **tcInd** only
- a blue laser light source (163-C12, Spectra Physics, Santa Clara CA) delivering typical 9 × 10^{-8} einstein s^{-1} cm^{-2} surfacic photon fluxes $\mathcal{I}_0$ at the illuminated sample. The laser typically delivers 15 mW at 488 nm. The laser beam was filtered through a LL01-488-25 laser cleanup filter (Semrock, Rochester, NY) and introduced with two mirrors (BB1-E02, Thorlabs, Newton, NJ) into a liquid light guide (LLG0338-4, Thorlabs). The exiting beam was collimated with a 50 mm focal lens. This blue laser light source was used for the blue illumination experiments involving both **tcInd** and 13-*cis*-RA
- a benchtop UV lamp (365 nm; essentially a 40 nm wide, at half height, Gaussian distribution centered at 350 nm; 6 W; Fisher Bioblock) delivering typical 3 × 10^{-8} einstein s^{-1} cm^{-2} surfacic photon fluxes $\mathcal{I}_0$ at the illuminated sample.

We checked that, when illuminated with these light sources at the time scale of our experiments, zebrafish embryos developed normally.

Experiments in Zebrafish Embryos. *General Information.* The transgenic line mp311+/+GFP has been reported in our previous work.[60] Fish were raised and bred according to standard methods.[65] The embryos were incubated at 28 °C. Developmental stages were determined as hours post fertilization (hpf).

Application of the Drugs. **Ind** and its caged precursor **cInd**, DEAB (diethylaminobenzaldehyde; Sigma-Aldrich), and *13-cis*-retinoic acid (13-*cis*-RA; Sigma-Aldrich) were solubilized at 10 mM in DMSO (those stock solutions were stored at −20 °C where they proved stable for several months). Aliquots of those solutions and (2-hydroxypropyl)-β-cyclodextrin 45% (w/v) in H_2O (Sigma-Aldrich) were added to Volvic water[66] containing the zebrafish embryos to reach the concentrations indicated in the text. Incubations were carried out in

dx.doi.org/10.1021/cb400178m | *ACS Chem. Biol.* 2013, 8, 1528−1536

the dark in plastic arrays of eight square 1.0 cm^2 fields (μ-Slides 8-well; Ibidi) containing 500 μL of solution and 10 zebrafish embryos.

en2-ER^{T2} Coding Plasmids. *myc-cEn2-ER^{T2}* coding plasmid: An intermediate vector (pC5fiERT) was first constructed by inserting Cre-ER^{T2} coding sequence (fragment XhoI-Ecl136I from pCre-ER^{T2}, a kind gift of D. Metzger and P. Chambon, Strasbourg, France [67]) into pcDNA5/FRT (Invitrogen, digested with XhoI and EcoO109I blunted with Klenow). We then prepared pC5fEn2ERT, with the coding sequence for *chicken En2* (*cEn2*), fused in N-ter to myc tag and in C-ter to ER^{T2} coding sequence, downstream CMV and T7 promoters and upstream the bovine growth hormone polyadenylation signal, via a trimolecular ligation between the NheI-*Hin*dIII fragment from pCL9mEn2,[68] pC5fiERT cleaved by NheI and XhoI, and a *Hin*dIII-XhoI adaptor. The final construct, **pCSmEn2ERT**, was built by transferring the NheI-XhoI fragment (NheI end blunted with Klenow enzyme) of pC5fEn2ERT into pCSgfpERT,[37,38] cleaved by BstBI (blunted with Klenow enzyme) and XhoI. **pCSmEn2ERT** contains the *myc-cEn2-ER^{T2}* coding sequence downstream simian CMV and SP6 promoters and upstream the late SV40 polyadenylation signal and was used to prepare synthetic RNA *in vitro* for injection in Zebrafish embryos. All conditions for restriction digests, gel purification, ligation and bacteria transformation are standard.[69] Plasmid complete sequences are available upon request.

Zebrafish Embryo Experiments. Zebrafish embryos were injected at one-cell stage with the synthesized mRNA (30 ng/μL) with an *in vitro* transcription kit (mMessage mMachine, Ambion). They were subsequently incubated in aqueous solutions of the various substrates according to the conditioning sequences reported in the main text. In the series of experiments devoted to orthogonal photoactivation of **tcInd** and 13-*cis*-RA, we first conditioned En2-ER^{T2} mRNA-injected mp311+/+GFP zebrafish embryos by incubating them with 10 μM DEAB (solution 1) from the sphere stage.[60] The embryos were subsequently transferred at 50% epiboly into a medium containing 10 μM DEAB and 5 nM 13-*cis*-RA (solution 2) for 5 min. They were then transferred into a medium containing 10 μM DEAB, 10 μM **tcInd**, and 10 μM (2-hydroxypropyl)-β-cyclodextrin (solution 3) in which they were incubated up to the photoactivation step: at 70% epiboly with 488 nm illumination for 5 min or/and at 90% epiboly with 365 nm illumination for 1 min, both durations being similar to photoactivation times. The zebrafish embryos were scored for their positive phenotype at 24 hpf (Figure 2a and Supplementary Figure 2S).[60] The results are shown in Supplementary Table 5S. Illuminated embryos were observed at 24, 48, and 72 hpf.

Quantification of the Positive Phenotypes. Zebrafish embryos were considered to exhibit a positive phenotype associated with overexpression of En2 when a reduction in eye size or completely missing eye(s) could be observed (see Figure 2). Zebrafish embryos were considered to exhibit a positive phenotype associated with 13-*cis*-RA photoactivation when a rescue of the green fluorescent rhombomere r5 was observed (see Supplementary Figure 2S). The percentage of positive phenotype was calculated as the ratio between the number of embryos exhibiting a positive phenotype to the total number of embryos.

Image Acquisition. The images of embryos were acquired using a spinning disk confocal microscope NIKON eclipse Ti equipped with a camera coll Snap HQ2 or a NIKON stereomicroscope SMZ1500.

■ ASSOCIATED CONTENT

Supporting Information

Syntheses (including Scheme 1S), the validation of the **Ind** inducer (including Table 1S), zebrafish embryo conditioning with the caged inducer **tcInd** (including Table 2S), the preliminary *in vivo* uncaging experiments (including Tables 3S and 4S), and the supplementary figures and tables. This material is available free of charge via the Internet at http://pubs.acs.org.

■ AUTHOR INFORMATION

Corresponding Author

*E-mail: Ludovic.Jullien@ens.fr.

Notes

The authors declare no competing financial interest.

■ ACKNOWLEDGMENTS

This work has been supported by the ANR (PCV 2008, Proteophane), the Ministère de la Recherche (a fellowship to L.F.), and the LEA-Nabi and the LIA CNRS-CNSI. The authors thank V. Jullien and G. Pons at Service de Pharmacologie Clinique, Saint Vincent de Paul Hospital Paris, for access to their HPLC−MS instrument, and Nicole Quenech'Du for technical help with the imaging platform.

■ REFERENCES

(1) Goeldner, M., and Givens, R., Eds. (2005) *Dynamic Studies in Biology*, 1st ed., Wiley-VCH, Weinheim.

(2) Mayer, G., and Heckel, A. (2006) Biologically active molecules with a light switch. *Angew. Chem., Int. Ed. 45*, 4900−4921.

(3) Ellis-Davies, G. C. R. (2007) Caged compounds: photorelease technology for control of cellular chemistry and physiology. *Nat. Methods 4*, 619−628.

(4) Young, D. D., and Deiters, A. (2007) Photochemical control of biological processes. *Org. Biomol. Chem. 5*, 999−1005.

(5) Lee, H.-M., Larson, D. R., and Lawrence, D. S. (2009) Illuminating the chemistry of life: Design, synthesis, and applications of caged and related photoresponsive compounds. *ACS Chem. Biol. 4*, 409−427.

(6) Specht, A., Bolze, F., Omran, Z., Nicoud, J.-F., and Goeldner, M. (2009) Photochemical tools to study dynamic biological processes. *HFSP J. 3*, 255−264.

(7) Yu, H., Li, J., Wu, D., Qiu, Z., and Zhang, Y. (2010) Chemistry and biological applications of photo-labile organic molecules. *Chem. Soc. Rev. 39*, 464−473.

(8) Deiters, A. (2010) Principles and applications of the photochemical control of cellular processes. *ChemBioChem 11*, 47−53.

(9) Brieke, C., Rohrbach, F., Gottschalk, A., Mayer, G., and Heckel, A. (2012) Light-controlled tools. *Angew. Chem., Int. Ed. 51*, 8446−8476.

(10) Klan, P., Solomek, T., Bochet, C. G., Blanc, A., Givens, R., Rubina, M., Popik, V., Kostikov, A., and Wirz, J. (2013) Photoremovable protecting groups in chemistry and biology: Reaction mechanisms and efficacy. *Chem. Rev. 113*, 119−191.

(11) Shestopalov, I. A., and Chen, J. K. (2008) Chemical technologies for probing embryonic development. *Chem. Soc. Rev. 37*, 1294−1307.

(12) Neveu, P., Aujard, I., Benbrahim, C., Saux, T. L., Allemand, J.-F., Vriz, S., Bensimon, D., and Jullien, L. (2008) A caged retinoic acid for use with one- and two-photon excitation in zebrafish embryos. *Angew. Chem., Int. Ed. 47*, 3744−3746.

(13) Baier, J., Maisch, T., Maier, M., Engel, E., Landthaler, M., and Baümler, W. (2006) Singlet oxygen generation by UVA light exposure of endogenous photosensitizers. *Biophys. J. 91*, 1452−1459.

(14) Kick, G., Messer, G., Plewig, G., Kind, P., and Goetz, A. E. (1996) Strong and prolonged induction of c-jun and c-fos proto-oncogenes by photodynamic therapy. *Br. J. Cancer 74*, 30−36.

(15) Klotz, L.-O., Pellieux, C., Briviba, K., Pierlot, C., Aubry, J.-M., and Sies, H. (1999) Mitogen-activated protein kinase (p38-, JNK-, ERK-) activation pattern induced by extracellular and intracellular singlet oxygen and UVA. *Eur. J. Biochem. 260*, 917−922.

(16) Wertz, K., Seifert, N., Hunziker, P. B., Riss, G., Wyss, A., Hunziker, W., and Goralczyk, R. (2006) β-Carotene interference with UVA-induced gene expression by multiple pathways. *Pure Appl. Chem. 78*, 1539−1550.

(17) At this point, one has to mention the alternative photoactivation approach explored by Falvey and his group. It relies on an electron

transfer from a photosensitizer molecule to a reducible protecting group leading to release of a substrate upon illuminating. In particular, visible-absorbing photosensitizers have been already used to control photorelease. See: (a) Sundararajan, C., and Falvey, D. E. (2005) *J. Am. Chem. Soc. 127*, 8000−8001. (b) Borak, J. B., López-Sola, S., and Falvey, D. E. (2008) *Org. Lett. 10*, 457−460. (c) Lee, K., and Falvey, D. E. (2000) *J. Am. Chem. Soc. 122*, 9361−9366.

(18) Gug, S., Bolze, F., Specht, A., Bourgogne, C., Goeldner, M., and Nicoud, J.-F. (2008) Molecular engineering of photoremovable protecting groups for two-photon uncaging. *Angew. Chem., Int. Ed. 47*, 9525−9529.

(19) Donato, L., Mourot, A., Davenport, C. M., Herbivo, C., Warther, D., Léonard, J., Bolze, F., Nicoud, J.-F., Kramer, R. H., Goeldner, M., and Specht, A. (2012) Water-soluble, donor-acceptor biphenyl derivatives in the 2-(*o*-nitrophenyl)propyl series: Highly efficient two-photon uncaging of the neurotransmitter aminobutyric acid at 800 nm. *Angew. Chem., Int. Ed. 51*, 1840−1843.

(20) Aujard, I., Benbrahim, C., Gouget, M., Ruel, O., Baudin, J. B., Neveu, P., and Jullien, L. (2006) *o*-Nitrobenzyl photolabile protecting groups with red-shifted absorption: Syntheses and uncaging cross-sections for one- and two-photon excitation. *Chem.—Eur. J. 12*, 6865−6879.

(21) Bao, C., Fan, G., Lin, Q., Li, B., Cheng, S., Huang, Q., and Zhu, L. (2012) Styryl conjugated coumarin caged alcohol: Efficient photorelease by either one-photon long wavelength or two-photon Nir excitation. *Org. Lett. 14*, 572−575.

(22) Chen, Y., and Steinmetz, M. G. (2005) Photochemical cyclization with release of carboxylic acids and phenol from pyrrolidino-substituted 1,4-benzoquinones using visible light. *Org. Lett. 7*, 3729−3732.

(23) Chen, Y., and Steinmetz, M. G. (2006) Photoactivation of amino-substituted 1,4-benzoquinones for release of carboxylate and phenolate leaving groups using visible light. *J. Org. Chem. 71*, 6053−6060.

(24) Sebej, P., Wintner, J., Müller, P., Slanina, T., Anshori, J. A., Antony, L. A. P., Klan, P., and Wirz, J. (2013) Fluorescein analogues as photoremovable protecting groups absorbing at 520 nm. *J. Org. Chem. 78*, 1833−1843.

(25) Zayat, L., Calero, C., Albores, P., Baraldo, L., and Etchenique, R. (2003) A new strategy for neurochemical photodelivery: Metal−ligand heterolytic cleavage. *J. Am. Chem. Soc. 125*, 882−883.

(26) Zayat, L., Salierno, M., and Etchenique, R. (2006) Ruthenium(II) bipyridyl complexes as photolabile caging groups for amines. *Inorg. Chem. 45*, 1728−1731.

(27) Furuta, T., Wang, S. S.-H., Dantzker, J. L., Dore, T. M., Bybee, W. J., Callaway, E. M., Denk, W., and Tsien, R. Y. (1999) Brominated 7-hydroxycoumarin-4-ylmethyls: Photolabile protecting groups with biologically useful cross-sections for two photon photolysis. *Proc. Natl. Acad. Sci. U.S.A. 96*, 1197−1200.

(28) Hagen, V., Frings, S., Wiesner, B., Helm, S., Kaupp, U. B., and Bendig, J. (2003) [7-(Dialkylamino)coumarin-4-yl]methyl-caged compounds as ultrafast and effective long-wavelength phototriggers of 8-bromo-substituted cyclic nucleotides. *ChemBioChem 4*, 434−442.

(29) Shembekar, V. R., Chen, Y., Carpenter, B. K., and Hess, G. P. (2005) A protecting group for carboxylic acids that can be photolyzed by visible light. *Biochemistry 44*, 7107−7114.

(30) Steer, R. P., and Ramamurthy, V. (1988) Photophysics and intramolecular photochemistry of thiones in solution. *Acc. Chem. Res. 21*, 380−386.

(31) Maciejewski, A., and Steer, R. P. (1993) The photophysics, physical photochemistry, and related spectroscopy of thiocarbonyls. *Chem. Rev. 93*, 67−98.

(32) Bhattacharyya, K., Das, P. K., Ramamurthy, V., and Rao, V. P. (1986) Triplet-state photophysics and transient photochemistry of cyclic enethiones, a laser flash photolysis study. *J. Chem. Soc., Faraday Trans. 2 82*, 135−147.

(33) Devanathan, S., and Ramamurthy, V. (1988) Photochemistry of α,β-unsaturated thiones: Cycloaddition of thiocoumarin to electron-rich and electron-deficient olefins from T_1. *J. Org. Chem. 53*, 741−744.

(34) Becker, R. S., Chakravorti, S., Gartner, C. A., and de Graca Miguel, M. (1993) Photosensitizers: Comprehensive photophysics/photochemistry and theory of coumarins, chromones, their homologues and thione analogues. *J. Chem. Soc. Faraday Trans. 89*, 1007−1019.

(35) Burdzinskia, G., Buntinx, G., Poizat, O., and Lapouge, C. (2005) Time-resolved resonance Raman investigation and ab initio calculations of the T_1-state structure of thiocoumarin. *J. Mol. Struct. 735−736*, 115−122.

(36) Fonseca, A. S. C., Soares, A. M. S., Goncalves, M. S. T., and Costa, S. P. G. (2012) Thionated coumarins and quinolones in the light triggered release of a model amino acid: synthesis and photolysis studies. *Tetrahedron 68*, 7892−7900.

(37) Sinha, D. K., Neveu, P., Gagey, N., Aujard, I., Benbrahim-Bouzidi, C., Saux, T. L., Rampon, C., Gauron, C., Goetz, B., Dubruille, S., Baaden, M., Volovitch, M., Bensimon, D., Vriz, S., and Jullien, L. (2010) Photocontrol of protein activity in cultured cells and zebrafish with one- and two-photon illumination. *ChemBioChem 11*, 653−663.

(38) Sinha, D. K., Neveu, P., Gagey, N., Aujard, I., Saux, T. L., Rampon, C., Gauron, C., Kawakami, K., Leucht, C., Bally-Cuif, L., Volovitch, M., Bensimon, D., Jullien, L., and Vriz, S. (2010) Photoactivation of the $CreER^{T2}$ recombinase for conditional site-specific recombination with high spatio-temporal resolution. *Zebrafish 7*, 199−204.

(39) Feil, R., Brocard, J., Mascrez, B., LeMeur, M., Metzger, D., and Chambon, P. (1996) Ligand-activated site specific recombination in mice. *Proc. Natl. Acad. Sci. U.S.A. 93*, 10887−10890.

(40) Brocard, J., Warot, X., Wendling, O., Messaddeq, N., Vonesch, J.-L., Chambon, P., and Metzger, D. (1997) Spatio-temporally controlled site-specific somatic mutagenesis in the mouse. *Proc. Natl. Acad. Sci. U.S.A. 94*, 14559−14563.

(41) Bochet, C. G. (2001) Orthogonal photolysis of protecting groups. *Angew. Chem., Int. Ed. 40*, 2071−2073.

(42) Kotzur, N., Briand, B., Beyermann, M., and Hagen, V. (2009) Wavelength-selective photoactivatable protecting groups for thiols. *J. Am. Chem. Soc. 131*, 16927−16931.

(43) Kantevari, S., Matsuzaki, M., Kanemoto, Y., Kasai, H., and Ellis-Davies, G. C. R. (2010) Two-color, two-photon uncaging of glutamate and GABA. *Nat. Methods 7*, 123−125.

(44) Goguen, D., Aemissegger, A., and Imperiali, B. (2011) Sequential activation and deactivation of protein function using spectrally differentiated caged phosphoamino acids. *J. Am. Chem. Soc. 133*, 11038−11041.

(45) Priestman, M., Sun, L., and Lawrence, D. S. (2011) Dual wavelength photoactivation of cAMP- and cGMP-dependent protein kinase signaling pathways. *ACS Chem. Biol. 6*, 377−384.

(46) Miguel, V. S., Bochet, C. G., and del Campo, A. (2011) Wavelength-selective caged surfaces: How many functional levels are possible? *J. Am. Chem. Soc. 133*, 5380−5388.

(47) Menge, C., and Heckel, A. (2011) Coumarin-caged dG for improved wavelength-selective uncaging of DNA. *Org. Lett. 13*, 4620−4623.

(48) Scheibye, S., Kristensen, J., and Lawesson, S.-O. (1979) Studies on organophosphorus compounds - XXVII1: Synthesis of thiono-, thiolo- and dithiolactones. *Tetrahedron 35*, 1339−1343.

(49) Gadre, J. N., Audi, A. A., and Karambelkar, N. P. (1996) New routes for the synthesis of some hydroxy 2H-1-Benzopyran-2-Thione derivatives. *Indian J. Chem. 35B*, 60−62.

(50) Yokoyama, M., Irie, M., Sujino, K., Kagemoto, T., Togo, H., and Funabashi, M. (1992) Thermal rearrangement of alkyl O-vinyl-carbohydroximates to 2-alkyloxazoles. *J. Chem. Soc., Perkin Trans. 1*, 2127−2134.

(51) Przychodzeń, W. (2005) Mechanism of the reaction of Lawesson reagent with N-alkylhydroxamic acids. *Eur. J. Org. Chem.*, 2002−2014.

(52) Schönleber, R. O., Bendig, J., Hagen, V., and Giese, B. (2002) *Bioorg. Med. Chem. 10*, 97−101.

(53) Stegmaier, P., Alonso, J. M., and del Campo, A. (2008) *Langmuir 24*, 11872−11879.

(54) Shi, Y., and Koh, J. T. (2004) Light-activated transcription and repression by using photocaged SERMs. *ChemBioChem 5*, 788−796.
(55) Nettles, K. W., Bruning, J. B., Gil, G., Nowak, J., Sharma, S. K., Hahm, J. B., Kulp, K., Hochberg, R. B., Zhou, H., Katzenellenbogen, J. A., Katzenellenbogen, B. S., Kim, Y., Joachimiak, A., and Greene, G. L. (2008) NFκB selectivity of estrogen receptor ligands revealed by comparative crystallographic analyses. *Nat. Chem. Biol. 4*, 241−247.
(56) Jaynes, J. B., and O'Farrell, P. H. (1988) Activation and repression of transcription by homoeodomain-containing proteins that bind a common site. *Nature 336*, 744−749.
(57) Scholpp, S., Lohs, C., and Brand, M. (2003) Engrailed and Fgf8 act synergistically to maintain the boundary between diencephalon and mesencephalon. *Development 130*, 4881−4893.
(58) Ando, H., Furuta, T., Tsien, R. Y., and Okamoto, H. (2001) Photo-mediated gene activation using caged RNA/DNA in zebrafish embryos. *Nat. Genet. 28*, 317−325.
(59) Ungos, J. M., Karlstrom, R. O., and Raible, D. W. (2003) Hedgehog signaling is directly required for the development of zebrafish dorsal root ganglia neurons. *Development 130*, 5351−5362.
(60) Xu, L., Feng, Z., Sinha, D., Ducos, B., Ebenstein, Y., Tadmor, A. D., Gauron, C., Saux, T. L., Lin, S., Weiss, S., Vriz, S., Jullien, L., and Bensimon, D. (2012) Spatiotemporal manipulation of retinoic acid activity in zebrafish hindbrain development via photo-isomerization. *Development 139*, 3355−3362.
(61) This value was retrieved from the data reported in ref 12.
(62) In this experiment, we turned to a filtered 488 nm strong light source to avoid the residual photoactivation of 13-*cis*-RA, which we observed with our nonfiltered 470 nm light source.
(63) Crosby, G. A., and Demas, J. N. (1971) Measurement of photoluminescence quantum yields. Review. *J. Phys. Chem. 75*, 991−1024.
(64) Wang, P. F., Jullien, L., Valeur, B., Filhol, J.-S., Canceill, J., and Lehn, J.-M. (1996) Multichromophoric cyclodextrins 5. Antenna-induced unimolecular photoreactions. Photoisomerization of a nitrone. *New. J. Chem. 20*, 895−907.
(65) Westerfield, M., Ed. (2000) *The Zebrafish Book: A guide for the laboratory use of zebrafish (Danio rerio)*, 4th ed., University of Oregon Press: Eugene, OR.
(66) Herbomel, P., Thisse, B., and Thisse, C. (1999) Ontogeny and behaviour of early macrophages in the zebrafish embryo. *Development 126*, 3735−3745.
(67) Feil, R., Wagner, J., Metzger, D., and Chambon, P. (1997) Regulation of Cre recombinase activity by mutated estrogen receptor ligand-binding domains. *Biochem. Biophys. Res. Commun. 237*, 752−757.
(68) Montesinos, M. L., Foucher, I., Conradt, M., Mainguy, G., Robel, L., Prochiantz, A., and Volovitch, M. (2001) The neuronal *Microtubule-Associated Protein 1B* is under homeoprotein transcriptional control. *J. Neurosci. 21*, 3350−3359.
(69) Ausubel, F. M., Ed. (1995) *Current Protocols in Molecular Biology*, Wiley, Weinheim.